

## Photolysis of Poly(*p*-methylstyrene)

N. A. WEIR, *Chemistry Department, Lakehead University,  
Thunder Bay, Ontario, Canada*

### Synopsis

Poly(*p*-methylstyrene) films have been irradiated with 253.7-nm radiation under high vacuum at 25°C. The main reaction product is hydrogen, but methane and traces of ethane and monomer were also detected. The quantum yield for H<sub>2</sub> production ( $6 \times 10^{-2}$ ) is considerably greater than that for polystyrene photolysis indicating that both  $\alpha$ -C—H bonds undergo fission. Solubility measurements also indicated the participation by the *p*-methyl group. Main-chain conjugation and coloration occur and are attributable to hydrogen abstraction from the  $\beta$ -carbon atom. Cyclohexadienyl compounds are also formed and are presumably associated with crosslinking involving addition to the benzene ring. The mechanisms of photochemical and photophysical processes are discussed.

### INTRODUCTION

The photochemistry of poly(*p*-methylstyrene) (PPMS) has been studied superficially by a number of investigators whose aim was to understand the deleterious effects of UV radiation on the performance of plastic scintillators based on polymers of methyl-substituted styrenes.<sup>1-3</sup> It has generally been established that exposure to shortwave UV radiation ( $\lambda = 254$  nm) results in a decreased fluorescence efficiency of the scintillator system attributable principally to photodegradation of the polymers.<sup>4</sup> However, several complicating factors associated with those systems have prevented a clear understanding of the photoprocesses involved. Most of the studies have been carried out in the presence of oxygen, and the observed effects are undoubtedly the results of simultaneous photodegradation and photo-oxidative degradations of the polymers. In addition, the scintillator systems contained small amounts of fluorescing solutes, like *p*-terphenyl, which could alter the course of photoreactions by acting as energy-transfer agents.

The purpose of the work described below was to make a systematic study of the photochemistry of PPMS. This work is part of an extended study of the general photochemical behavior of polystyrene and its derivatives.<sup>5</sup> In order to prevent concurrent photo-oxidation, reactions were carried out under high vacuum conditions or in the presence of oxygen-free gases which were considered inert toward free radicals and other possible intermediates.

## EXPERIMENTAL

### Polymer Preparation

Polymers were prepared to 15% conversion in bulk in the presence of AIBN (0.05%) and thermally at 80°C. The monomer (K & K Laboratories) was purified by washing with dilute KOH and water and dried for 16 hr over anhydrous MgSO<sub>4</sub>. It was then distilled under reduced pressure in the presence of nitrogen, the middle fraction only (bp 67–68° at 36 mm Hg) being retained. Gas-chromatographic analyses showed the fraction to be pure, and isomeric impurities were, according to the suppliers, present to an extent of less than 0.1%. The purified samples were degassed and stored under high vacuum in a light-proof reservoir until required. Polymerization was carried out under high vacuum conditions at 80° ± 0.1°C in dilatomers which were filled by molecular distillation of the monomer from the reservoir, and the polymer was isolated by precipitation, the toluene solution of the polymer and unreacted monomer being added to the methanol. Precipitation was repeated three times, and the polymer was dried and stored under high vacuum conditions.

### Molecular Weight Determination

This was carried out at 37°C using a Mechrolab 501 osmometer with toluene as solvent.

The two polymers studied had the characteristics shown in Table I.

TABLE I  
Characteristics of Polymers Studied

Polymerization temp., °C	$\bar{M}_n$	AIBN, %
80	410,000	0.00
80	192,000	0.05

### Film Preparation

Polymers were irradiated in the form of thin films which were cast from toluene solution on a clean mercury surface. The films were subsequently pumped for several days at 10<sup>-5</sup> mm Hg, and no experiments were undertaken until they were freed from toluene, the presence of residual toluene in the films being indicated by mass spectrometry. The film thickness used throughout was 0.005 mm.

It is obviously desirable in a study like this to use very thin films to avoid diffusion-controlled reactions; on the other hand, the films have insufficient mechanical strength, and the two requirements are to some extent mutually exclusive. However, diffusion measurements indicated that although it required very careful handling, a 0.005-mm-thick, with a maximum diffusion path of 0.0025 mm in this experimental setup, was sufficiently thin to prevent formation of gaseous products becoming a diffusion-controlled

process, the rate of diffusion of H<sub>2</sub> through it being at least an order of magnitude higher than its rate of product on by photolysis.<sup>6</sup>

### Photochemical Techniques

The films were mounted in stainless steel holders and placed in a demountable fused silica vessel which was connected via a ground joint to a mercury-free vacuum system, the vacuum being indicated by an ionization gauge sealed into the reaction vessel. Polymer films were degassed until a constant pressure was obtained and then irradiated at 30°C under high vacuum (10<sup>-6</sup> mm Hg) and in the presence of various amounts of "inert" gases, argon, CO<sub>2</sub>, and N<sub>2</sub>, the pressures of these gases being indicated by a pressure transducer (Bourne Model 410).

The UV source was a low-pressure Hg arc (Ultra Violet Products, Model PCQX1) which, according to manufacturer's specification, emits at least 98% of its radiation at 253.7 nm. Light from the arc was focused by means of a quartz lens into a parallel beam which transversed the reaction vessel. The fraction of light absorbed by a film was determined using a phototube (R.C.A. Type 1P28), the output of which was monitored with a microvoltmeter (Keithley Model 155).

It was established that the absorption characteristics of the films at 253.7 nm could be represented by the Beer-Lambert law,  $I = I_0 e^{-\mu L}$  where  $I$  and  $I_0$  are the transmitted and incident intensities, respectively,  $\mu$  is the absorption coefficient, and  $L$  is the thickness ( $\mu = 1.8 \times 10^3 \text{ cm}^{-1}$ ).

The quantum output at 253.7 nm was determined by ferrioxalate actinometry,<sup>7</sup> and the incident intensity was  $1.3 \times 10^{-9} \text{ E cm}^{-2} \text{ sec}^{-1}$ .

### Soluble Fraction Determination

After irradiation, films were dissolved in toluene and the insoluble gel fraction was removed by centrifugation. After several washings with toluene, it was dried and weighed. The soluble fraction was determined, after solvent evaporation, by weighing.

### Gas Analyses

Instantaneous pressure changes occurring in the reaction vessel as a result of irradiation were observed on the ionization gauge.

After irradiation, the gases were pumped out of the reaction vessel by means of a mercury-free Toepler-type pump which incorporated Teflon and ground-glass seals and which was operated electrically by means of solenoids. The gases were transferred quantitatively to a trap immersed in pumped liquid N<sub>2</sub> (-205°C), transfer being indicated by the ionization gauge. The mixture was thus divided into two fractions, one condensable at -205°C and the other, noncondensable. Each fraction was then transferred quantitatively to a gas chromatography injection loop from which it was flushed directly onto the column by carrier gas. The noncondensable fraction was analyzed on a 2-meter molecular sieve (5A, 60 mesh) column

at 30°C. N<sub>2</sub> was the carrier gas, and the detector was a katharometer. The condensable fraction was separated on a 1-meter Poropak R column at 100°C using He as a carrier gas and a flame ionization detector. The columns were calibrated for all the gases using pure samples. The nature of the products was confirmed by mass spectrometry, small portions of the column effluents being introduced directly to the RMU7 mass spectrometer.

### Spectra

Spectra of films undergoing degradation were obtained by irradiating them in fused silica spectroscopy cells fitted with demountable stopcocks. Using this technique, it was possible to measure spectral changes continuously without having to remove the films from the irradiation environment (vacuum, etc.) and hence expose them to atmospheric oxygen.

Infrared spectra were obtained using a Beckman IR12 spectrometer; UV and visible, using a Perkin Elmer 402 spectrometer; and fluorescence spectra, using a Perkin Elmer 203 fluorimeter.

## RESULTS AND DISCUSSION

### Volatile Products

Instantaneous pressure changes were obtained during irradiation of films; Figure 1 is typical of the results obtained. It can be seen that gas evolution is associated with irradiation. No pressure changes were observed when the apparatus was irradiated in the absence of a film. Gas evolution appears to be linear with time for a period of about 40 min, after which it decreases progressively with time.

Analyses showed that hydrogen was the major product, but small amounts of methane, ethane, and traces of styrene, *p*-methylstyrene, and toluene were also obtained. It is conceivable that some of the toluene is associated with residual solvent in the polymer, toluene having a high tenacity for styrene polymers.<sup>8</sup>

Figure 2 shows that although the rate of H<sub>2</sub> evolution is constant over the first 70 min, the rate of methane formation decreases after a short time. This behavior parallels the total pressure changes (Fig. 1), and it is unlikely that it is due to depletion of the polymer since the total volatile evolution corresponds to less than 1% decomposition.

It is more likely that the rates of formation of the products are governed by their rates of diffusion out of an increasingly crosslinked polymer matrix. On account of its small volume, the H<sub>2</sub> molecule will be relatively unaffected, particularly when the crosslink density is not high. Also shown in Figure 2 are results obtained at 55°C, and it can be seen that in the early stages of the reaction, the rate of methane formation coincides with that obtained at 30°C; and this rate is maintained for about 1 hr after which

curvature is observed. It is possible, therefore, that diffusion of  $\text{CH}_4$  through the crosslinked polymer has a higher activation energy than that associated with unreacted polymer. The increased yield of  $\text{CH}_4$  at  $55^\circ\text{C}$  is possibly also partly due to greater participation of transfer reactions.

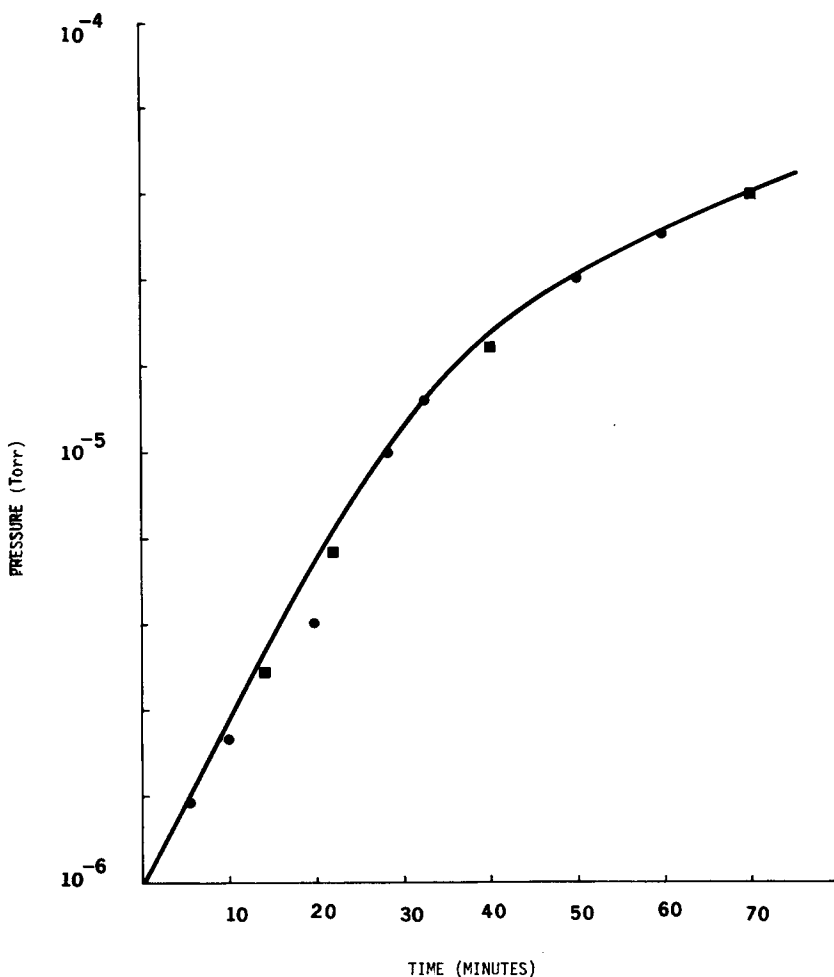


Fig. 1. Pressure changes in the reaction vessel as a function of time of vacuum irradiation at 253.7 nm: (●) thermal polymer; (□) AIBN-initiated polymer.

It is also possible that the coloration of the polymer which accompanies volatile evolution contributes to decreased photolysis rates, the yellow surface layers acting as an internal UV filter protecting the bulk of the film. It can also be concluded from Figure 2 that the photolysis reactions are not sensitive to the presence of nitrile endgroups on the chains, the rates of the product evolution being indistinguishable (within experimental error) for the two polymers.

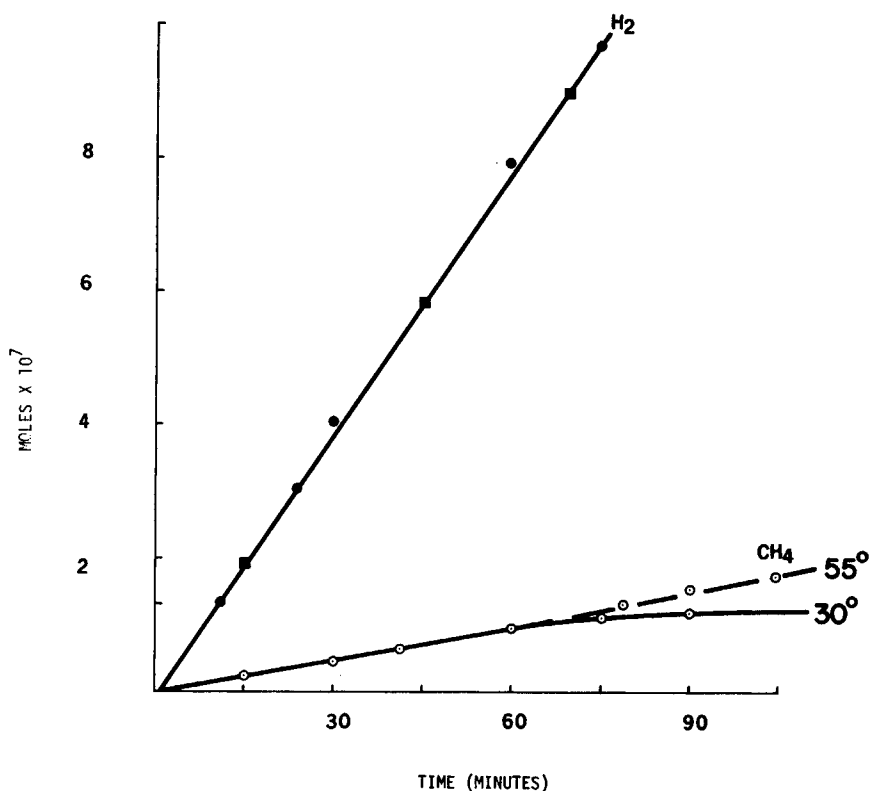


Fig. 2. Progress curves for volatile product formation. Vacuum irradiation of PMMS at 253.7 nm: (●) thermal polymer; (□) AIBN-initiated polymer.

### Light Intensity

Ultraviolet intensities were varied by varying the arc-film distance and by interposing actinometrically calibrated brass intensity screens between the film and arc, and the effect of intensity on  $H_2$  production was studied. The results are shown in Table II, where rates are expressed as moles  $H_2$  per

TABLE II  
Vacuum Photolysis of PPMS at 253.7 nm:  $H_2$  Formation as a Function of UV Intensity at 30% (0.005 mm Film)

Rate of $H_2$ production R, $\mu$ moles/mole polymer sec	Relative intensity $I_0$ , %	$R/I_0$
31	100	0.31
27.8	81.7	0.34
20.9	64.3	0.32
15.1	45.6	0.33
9.9	32.2	0.31
6.7	22.1	0.30
0.32	10.0	0.32

mole polymer per sec. This is essentially an average value based on the rate of photolysis of a  $5 \times 10^{-4}$ -cm-thick film. Reaction times were kept to a minimum to avoid complications due to secondary reactions.

It can be seen that the rate  $R$  is proportional to the rate of absorption of 253.7 nm radiation and hence to the incident intensity, i.e.,  $R = \phi_{\text{H}_2} I_0^\chi (1 - e^{-\mu L})$ , where  $\chi$  is the intensity exponent and  $\phi_{\text{H}_2}$  is the quantum yield for  $\text{H}_2$  formation. The actual value of this intensity exponent, determined from this log-log plot of the data in Table II, is 1.24.

Because of the high extinction coefficient, 253.7 nm, radiation is non-uniformly absorbed throughout the films. The treatment used to calculate the quantum yield is modified as follows: If the light absorbed in an elementary layer of polymer of thickness  $dL$  and distance  $L$  from the surface on which the light is incident is  $dI$  (quanta  $\text{cm}^{-2} \text{sec}^{-1}$ ) and  $I_0$  is the incident intensity, then

$$\frac{dI}{dt} = I_0 e^{-\mu L} \text{ (from Beer's law).}$$

The rate of light absorption in quanta per unit thickness per unit time is

$$\frac{dI}{dt} = I_0 e^{-\mu L}.$$

The total number of quanta absorbed by a film of thickness  $L$  is  $I_a$ , and

$$\begin{aligned} I_a &= \frac{1}{L} \int_0^L (I_0 e^{-\mu L}) dL \\ &= \frac{1}{L} [I_0(1 - e^{-\mu L})]. \end{aligned}$$

The quantum yield for product formation  $\Phi$  is

$$\Phi = \frac{\text{net rate of formation of product in film}}{\text{mean rate of absorption of quanta}}.$$

In this case,  $dX/dt \propto I_a$  to the first power. Hence,

$$\begin{aligned} \Phi &= \frac{dX}{dt} \frac{1}{I_a} \\ &= \frac{dX}{dt} \frac{L}{I_a(1 - e^{-\mu L})}. \end{aligned}$$

Quantum yields were calculated using this equation, and the following values were obtained:

$$\Phi_{\text{H}_2} = 6 \times 10^{-2}$$

$$\Phi_{\text{CH}_4} = 3.5 \times 10^{-4} \text{ (based on linear part of the curve)}$$

$$\Phi_{\text{C}_2\text{H}_6} = 1.1 \times 10^{-4} \text{ (determined mass-spectrometrically)}$$

Values of  $\Phi$  of these orders of magnitude are typical of polymer photolysis reactions, indicating that electronic energy is efficiently dissipated and that product formation involving chain reactions is unlikely. However, the value of  $\Phi_{H_2}$  is greater than that obtained under identical conditions of polystyrene<sup>5</sup> ( $\Phi_{H_2} = 3.5 \times 10^{-2}$ ) by a factor of almost 2, suggesting that C—H bond fission in the *p*-methyl group is an additional source of  $H_2$ . The resulting free radical would be as stable, if not more stable (considering steric effects), than that formed by  $\alpha$ -C—H fission. This theory is supported by the findings of Burlant<sup>9</sup> who estimated that the *p*-substituent in alkyl-substituted polystyrenes was the source of approximately half the  $H_2$  yield during  $\gamma$ -radiolysis of these polymers.

### Solubility Measurements

Insolubilization is concomitant with volatile formation, the fraction of insoluble gel increasing with exposure for about 1 hr, after which it decreases rapidly. At this stage, the polymer is highly crosslinked, and the macroradicals have little mobility, however, volatile formation is still possible on account of the greater mobilities of the small-radical precursors.

The data were analyzed using Charlesby's<sup>10</sup> equation which is applicable to simultaneous chain scission and crosslinking of a polymer having an initial random molecular weight distribution:

$$S + S^{1/2} = \frac{\alpha}{\beta} + \frac{1}{\beta P_0 D}$$

in which  $S$  is the weight of the soluble portion after absorbance of a radiation dose  $D$ ,  $P_0$  is the initial number-average degree of polymerization, and  $\alpha$  and  $\beta$  are constants proportional to the probabilities of chain scission and crosslinking, respectively. This equation has been found to represent photochemical degradation adequately<sup>11,12</sup> when modified to

$$S + S^{1/2} = \frac{\alpha}{\beta} + \frac{1}{P_0 \beta I_0 t}$$

where  $I_0$  is the incident intensity and  $t$  is the time of irradiation. Figure 3A is a typical plot of  $(S + S^{1/2})$  versus  $t^{-1}$ . It can be seen then as the reaction proceeds, there is progressive departure from linearity, however extrapolation of the linear portion to zero dose gives an intercept of  $\alpha/\beta = 0.26$ , indicating that crosslinking is almost four times more probable than chain scission. This ratio is considerably lower than that observed for polystyrene,<sup>13</sup> i.e., 0.42, and it reflects the ease of crosslinking of PMMS, the *p*-methyl group presumably being capable of participating in the crosslinking. The departure from linearity is probably associated with the changes in absorption characteristics due to coloration of the polymer; similar behavior has been observed for poly(vinyl chloride).<sup>14</sup> Figure 3B shows similar results obtained at 90°C. It can be seen that the extent of scission increases considerably, and this cannot be due to thermal degradation since



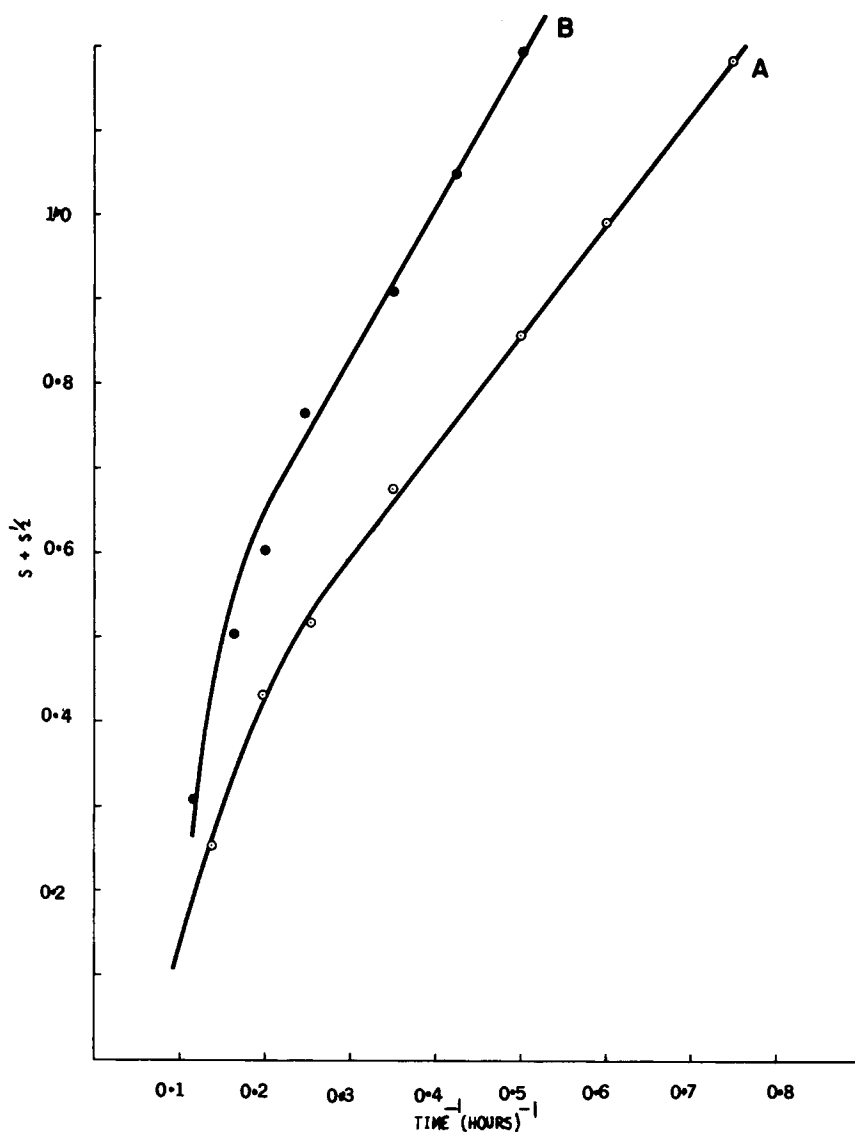


Fig. 3. Charlesbey plots of soluble fractions vs. reciprocal exposure times to 253.7-nm radiation: (A) reaction at 25°C; (B) reaction at 90°C; both under high vacuum.

PMMS is stable to at least 250°C. The temperature is close to the  $T_g$  value (100°C), and the results imply that the onset of segmental motion facilitates the separation of the fragments formed on chain scission. These are formed initially in a cage, and most will recombine since escape from the cage will involve some diffusive or rotational displacement which will be greatly impeded by the high viscosity of the solid polymer.

Molecular weight measurements were carried out in the soluble fractions of the films, thus  $M_n$  values after 30 min of irradiation being  $3.1 \times 10^5$  and

$1.4 \times 10^5$  for the two polymers, indicating that chain scission was definitely occurring.

An estimate of the apparent quantum yield for chain scission  $\Phi_s$  can be made from these figures, assuming that the rate is constant and that crosslinking is not involved in the soluble portion:

$$\Phi_s = \frac{W \partial \left[ \frac{(\bar{M}_n)_0}{(\bar{M}_n)_t} - 1 \right]}{(\bar{M}_n)_0 \partial [I_a]}$$

where  $(\bar{M}_n)_0$  and  $(\bar{M}_n)_t$  are the number-average molecular weights initially and after time of irradiation,  $W$  is the weight of sample, and  $I_a$  is the intensity of light absorbed. Values of  $\Phi_s = 1.3 \times 10^{-4}$  and  $9.8 \times 10^{-5}$  are obtained for the thermal and AIBN-initiated polymers; the difference in these figures is not considered significant.

The reaction profile through the polymer was investigated using stacks of films 0.0030 nm thick. The individual films were not sufficiently strong mechanically to withstand irradiation, but when firmly clamped in a stack were satisfactorily strong. After irradiation (20 min), the films were separated and the insoluble portions of each analyzed. It can be seen that the extent of radical formation, as reflected by crosslinking is a function of 253.7-nm radiation penetration. The rate of insolubilization is proportional to the rate of radical formation, hence the fraction of insoluble material  $F$  formed in a film of thickness  $L$  in a given time will be proportional to the amount of light absorbed by the film for the initial part of the crosslinking (before multiple crosslinking, etc., occurs), i.e.,

$$F \propto I_0(1 - e^{-\mu L}).$$

For the first film with incident intensity  $I_0$  falling on it,

$$F = \Phi_c I_0(1 - e^{-\mu L})$$

where  $\Phi_c$  is the quantum yield for crosslinking. The incident intensity on the second film of thickness  $L$  is  $I_0 e^{-\mu L}$ . Thus,

$$F_2 = \Phi_c I_0 e^{-\mu L} (1 - e^{-\mu L}).$$

In general, the insoluble fraction for a given film in the stack is  $F_n$ ,

$$F_n = \Phi_c I_0 e^{(n-1)\mu L} (1 - e^{-\mu L}).$$

This predicts the semilogarithmic relation between  $F$  and the number of films (or thickness), which is shown on Figure 4.

### Spectral Changes

**U.V.** The U.V. spectrum shows little change except in the 238-nm region, where a new band appears on irradiation. Similar results were obtained for polystyrene, (5) and the absorption was attributed to main-chain unsaturation, the 200-nm band due to the phenylic segments being perturbed by the adjacent unsaturation.

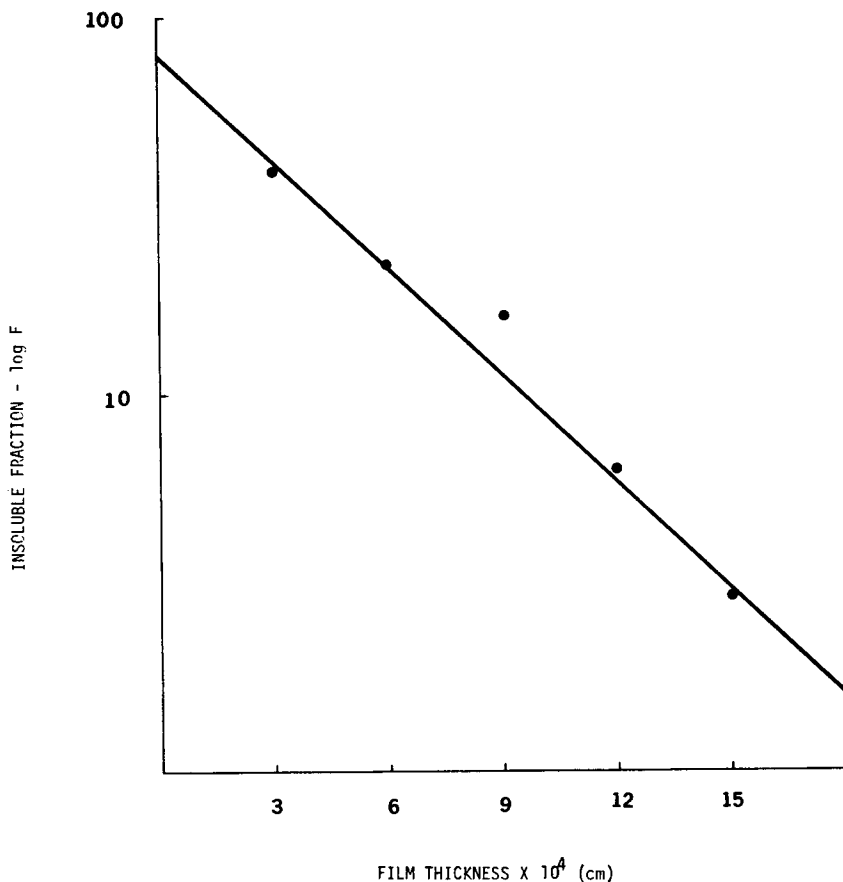


Fig. 4. Insoluble fraction  $F$ , per 0.003-mm film thickness (semilogarithmic plot) Vacuum irradiation of PMMS at 253.7 nm.

**Visible.** Yellowish discoloration is also associated with irradiation, a progressive increase in absorption at 440 nm being observed. This behavior is also reminiscent of polystyrene and is indicative of the presence of main-chain conjugated sequences. The general characteristics of formation of these chromophores are shown in Figure 5, the shape of which can be explained in terms of photolysis of the chromophores and/or self-inhibition, the colored surface material absorbing the radiation and protecting lower layers.

Photolyses were carried out in presence of added gases ( $O_2$ -free  $CO_2$  and  $N_2$ ). The results are shown in Figure 6, where it can be seen that the presence of gas which does not participate in photolyses favors mainchain unsaturation. It is interesting to note that while the positions of the maxima in the UV and visible spectra are not significantly changed on prolonged irradiation, the intensities are increased, and it is concluded that geometrical requirements for extended conjugation (which would lead to

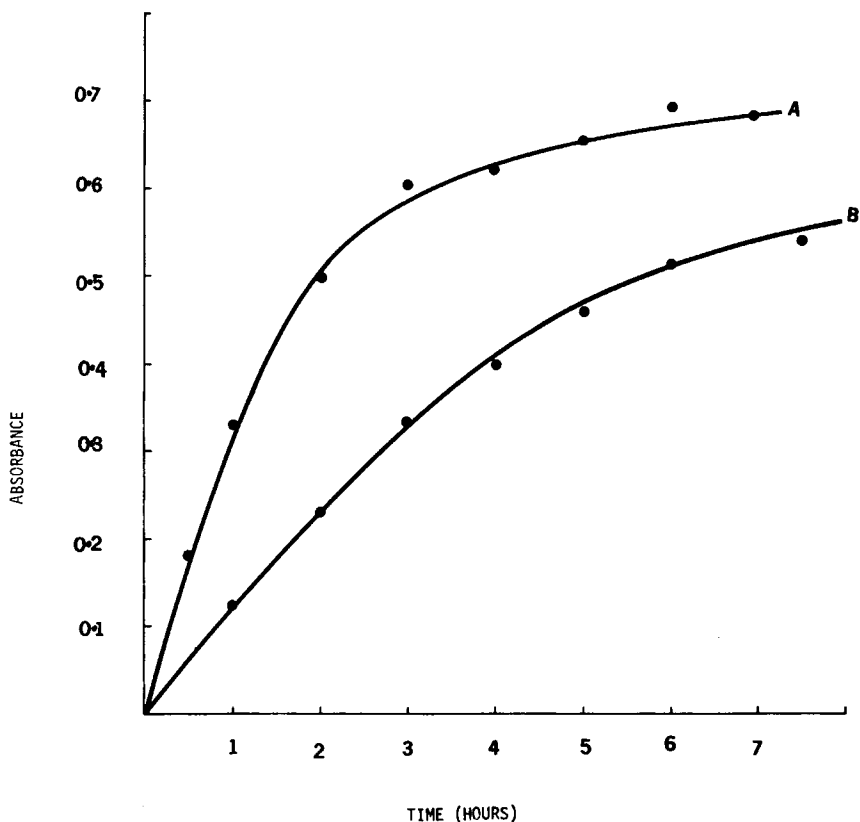


Fig. 5. Characteristics of chromophore formation during vacuum irradiation of PMMS: (A) absorbance at 238 nm; (B) absorbance at 440 nm.

bathochromic shifts of maxima) cannot be met owing to interference from crosslinking.

**Fluorescence.** The fluorescence spectrum of a PMMS film excited with 253.7-nm radiation consists of two bands, a low-intensity one at 285 nm and a broader, higher-intensity band with a maximum at 335 nm. The former is due to the phenylic segments, and the latter is caused by excimer fluorescence. The effects of radiation of PMMS on the fluorescence yields are shown in Figure 7, in which the relative fluorescence intensities (no irradiation representing 100% yield) are shown as a function of exposure of the films to UV.

It can be seen from curves C + D that the excimer fluorescence is much more sensitive to the effect of polymer degradation. Several factors may account for these effects:

(a) *Coloration:* As the polymer becomes discolored on irradiation, the intensity of exciting radiation (strongly absorbed) will be attenuated on traversing the surface layers of the films, with consequent decreases in fluorescence intensities. The contribution of the filter effect can be as-

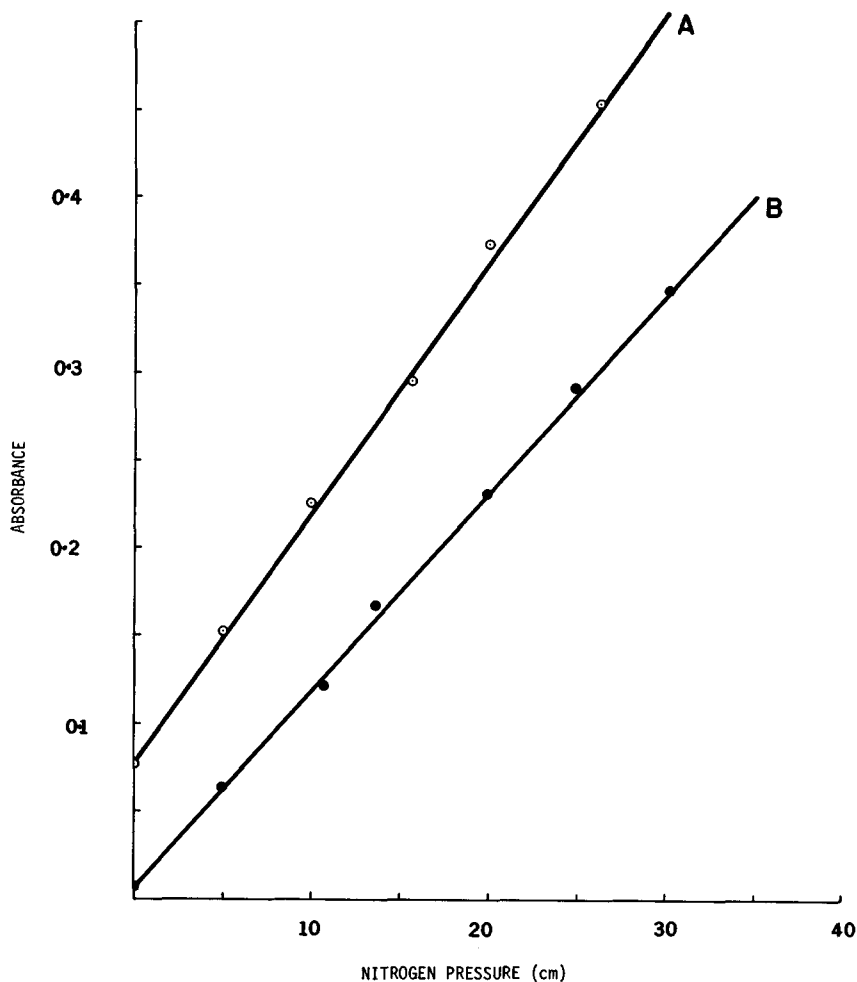


Fig. 6. Irradiation of PMMS at 253.7 nm in presence of  $O_2$ -free nitrogen. Absorbance after 2 hr of irradiation as a function of  $N_2$  pressure: (A) 238 nm absorbance; (B) 440 nm absorbance.

sessed from Figure 5 and an appropriate correction made; however, it was found that the effect was small and certainly not sufficient to account for Figure 7.

(b) *Quenching*: Two types can be recognized, color and chemical quenching. It is highly probable that color quenching will be involved, the fluorescent radiation being absorbed by the colored film. Chemical quenching will be more important, however, and can arise as a result of energy transfer from the initially excited phenylic segments to the adjacent conjugated systems in the main chain (formed by UV irradiation), a process which will compete with the intramolecular excimer foundation.

(c) *Geometry*: The importance of geometric and steric factors in controlling excimer formation has been emphasized by several previous

workers.<sup>15,16</sup> For example, the excimer band disappears from the spectrum of polystyrene when the polymer is frozen into a rigid glass at 77°K,<sup>17</sup> and it was suggested that at that temperature there is insufficient molecular motion to allow proper alignment of adjacent chromophores. Fox<sup>18</sup> has distinguished two types of energy transfer to form the excimer, a singlet-energy migration involving several segments and a transfer of energy from the singlet to an adjacent segment.

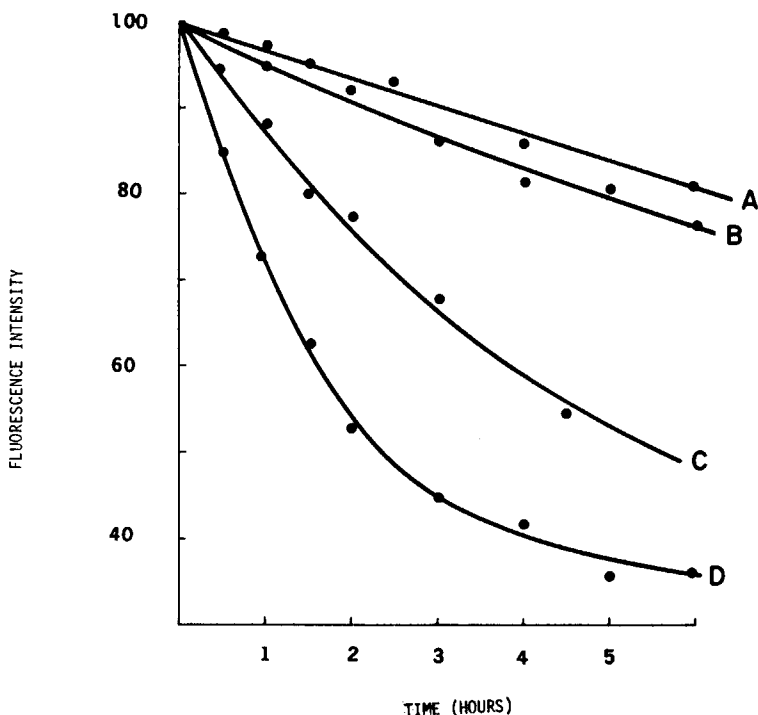


Fig. 7. Fluorescence intensities as a function of time of vacuum irradiation of PMMS at 253.7 nm: (A) singlet fluorescence (285 nm) at 25°; (B) singlet fluorescence (285 nm) at 85°; (C) excimer fluorescence (335 nm) at 85°; (D) excimer fluorescence (335 nm) at 25°.

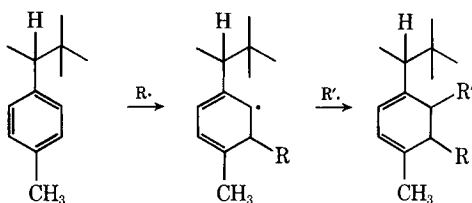
It is possible that crosslinking makes the system sufficiently rigid to reduce the probability of a number of segments attaining favorable orientations with respect to each other, and the optimum conditions for energy transfer cannot be maintained. If this energy cannot be transferred intramolecularly, it is reasonable to expect that the intensity of fluorescence of the phenylic segments will increase, since excimer concentrations increase with increased molecular mobility. However, studies with unirradiated films at 85°C show that while the decrease in segmental fluorescence intensity is comparable with the difference between curves A and B (Fig. 7), the increase in excimer fluorescence is less than half the difference between curves C and D. It can thus be concluded that partial relaxation of the

rigid structure at 85°C makes excimer formation possible again. These results also show the considerable contribution of crosslinking to the decreased excimer fluorescence intensity.

**IR Spectra.** Changes in IR spectra were observed in three regions. Shoulders appeared at 820  $\text{cm}^{-1}$  on the 840  $\text{cm}^{-1}$  and 700  $\text{cm}^{-1}$  bands, respectively, and a low-intensity absorption appeared at 895  $\text{cm}^{-1}$ .

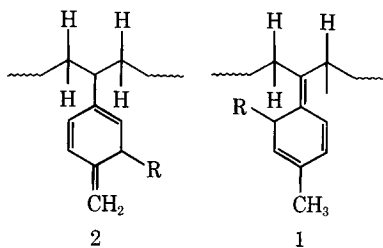
These absorptions are characteristic of olefins of the type  $\text{RCH}=\text{CR}_2$  (808–835  $\text{cm}^{-1}$ ), *cis*- $\text{RCH}=\text{CHR}_1$  (675–720  $\text{cm}^{-1}$ ), and  $\text{RCR}_1=\text{CH}_2$  (885–890  $\text{cm}^{-1}$ ),<sup>19</sup> the last mentioned moving to 895  $\text{cm}^{-1}$  in the presence of conjugation.<sup>20</sup> These absorptions may be rationalized in terms of the following reactions.

(a) Addition of a micro- or macroradical to the benzene ring followed by a subsequent addition to the resulting radical to form a cyclohexadiene:



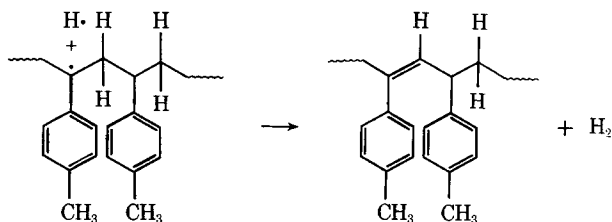
Addition of large fragments would constitute crosslinking.

(b) Addition of a micro- or macroradical to a canonical form of the primary radical:



Similar mechanisms of crosslinking involving benzene rings have been previously suggested.<sup>21</sup>

The 895  $\text{cm}^{-1}$  absorption is probably associated with the *p*-methyl group participation (structure 2). Main-chain unsaturation can be envisaged as follows (the mechanism of its formation is discussed below):



## The Reaction Mechanism

### *Primary Processes*

The UV spectrum of PMMS consists of a broad band (245–275 nm) with a maximum at 265 nm. The band is associated with excitation of the electrons in the phenyl groups. The initially formed species will be an excited singlet which can be deactivated by a number of photophysical and photochemical processes. A large amount of energy will be lost by a radiationless internal conversion to the ground state and by singlet fluorescence. Excimer formation has been observed, and triplet formation will also occur. The remaining energy will be partitioned among the photodissociation process. The energies corresponding to these excited states are as follows: singlet, 101 kcal/mole; excimer, 85 kcal/mole; and triplet, 83 kcal/mole. The small splitting between excimer and triplet will ensure population of the triplet levels.

In order to account for the gaseous products and for chain scission, C—H and C—C bond fissions must be invoked. Neither of these bonds absorbs UV radiation directly; consequently fission must be brought about by energy transfer from the excited phenyl groups. The energy requirements for these fissions are not known, but plausible values for the dissociation energies of various bonds in the molecule may be calculated using Benson's methods.<sup>22</sup> The following values are obtained:  $\alpha$ -C—H, 80 kcal/mole; C—H (*p*-methyl group), 84 kcal/mole; C—CH<sub>3</sub>, 88 kcal/mole; C—C (main chain), probably about 80 kcal/mole. It can thus be seen that the singlet state has associated with it sufficient energy to bring about fission of all of these bonds, provided that the appropriate energy transfer occurs; but reaction from the triplet will likely be restricted to  $\alpha$ -C—H, main chain and perhaps C—H (*p*-methyl) fissions.

It has been established that  $\alpha$ -C—H fission occurs in polystyrene, and it is reasonable to expect PMMS to behave similarly. However, the *p*-methyl group is also in the  $\alpha$ -position, and the enhanced rate of H<sub>2</sub> production over polystyrene indicates that C—H fission is also occurring in the *p*-CH<sub>3</sub> group. The formation of CH<sub>4</sub> indicates that C—CH<sub>3</sub> fission is occurring; the low yield may be attributed to the participation of only the singlet state.

Chain scission presumably occurs from both singlet and triplet levels. The energetics of these reactions are shown in Figure 8.

The quantum yields for all of these bond fissions are typically low (for polymer systems), and this is generally attributed to the effective competition from the various photophysical processes. However, the radicals are formed initially in cages in which geminate recombination occurs at the expense of diffusive escape from the cages, the effective viscosity of the solid film being high.

### *Secondary Reactions*

These are the results of the interactions of micro- and macroradicals and of the reactions of radicals with the polymer, the most important being H<sub>2</sub> production and crosslinking.

Hydrogen may be formed by the direct combination of two atoms (in presence of a third body), but on account of the reactivity of H atoms



it is likely that most of the molecular hydrogen results from inter- and intramolecular hydrogen abstraction reactions. Abstraction from the  $\alpha$ -position of a neighboring chain seems very probable, but intramolecular abstraction from the  $\beta$ -position (i.e., the atom adjacent to the initial C—H fission) which has been shown to account for main-chain unsaturation in polystyrene would appear to be equally probable with PMMS. When the initial C—H fission occurs from the singlet state, the polymer radical will be considerably excited, and this will facilitate the elimination reaction. The progress of this reaction is illustrated in Figure 8.

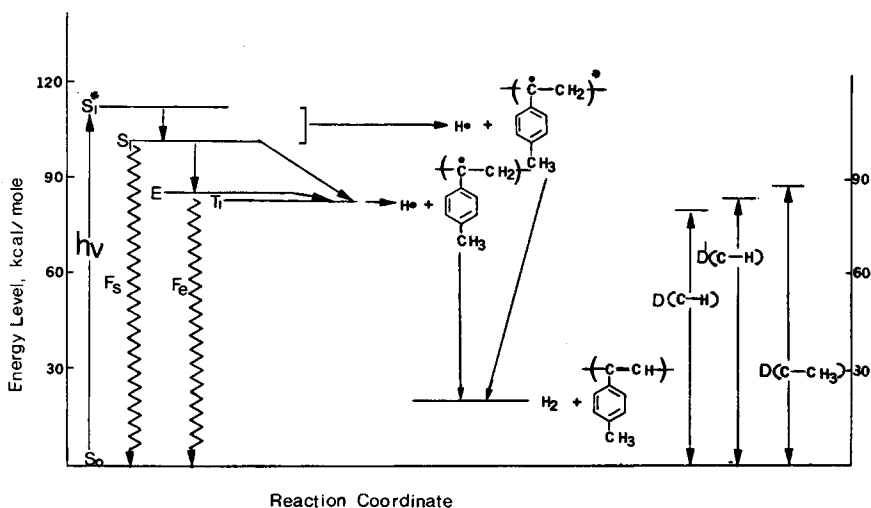


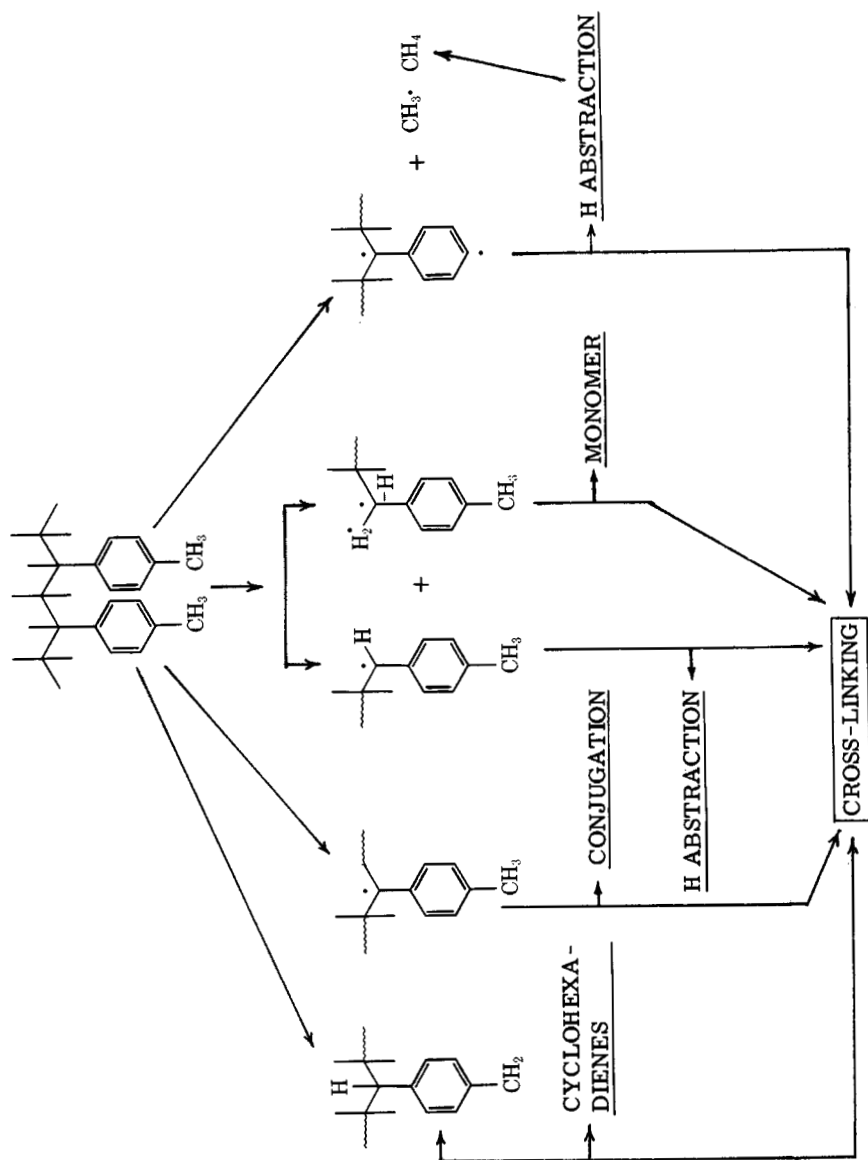
Fig. 8. Energy levels in PMMS and relevant bond dissociation energies. Progress of hydrogen elimination reaction: (S) singlet; (E) excimer; (T) triplet; ( $F_s$ ,  $F_F$ ) singlet and excimer fluorescence;  $D(\text{C—H})$ ,  $D(\text{C—H})$ , and  $D(\text{C—CH}_3)$ , dissociation energies of the  $\alpha$ -C—H, the *p*-methyl C—H, and the phenyl—CH<sub>3</sub> bonds, respectively; (wavy) radiative transitions; (solid) Nonradiative transitions.

When the reactions are carried out in presence of added gases, N<sub>2</sub> and CO<sub>2</sub>, the H atom mobilities are considerably diminished, and some of the atoms which would otherwise have diffused away from their region of formation are available for abstraction of H atom from the  $\beta$ -position, with a consequent enhancement of conjugation and coloration shown in Figure 6.

The value of the intensity exponent (1.24) indicates that H<sub>2</sub> production is predominately a monophotonic process, as would be predicted for both inter- and intramolecular H abstractions. The value is perhaps sufficiently greater than one to suggest that some direct recombination of H atoms also occurs.

Methane will result from similar abstraction reactions involving the methyl radical, and direct union of H atoms and CH<sub>3</sub> radicals will perhaps also occur. The presence of small yields of ethane suggests that a small amount of methyl-radical combination occurs, since it is highly unlikely that a methyl radical is abstracted.

The most important reactions occurring are summarized in the following scheme:



The author gratefully acknowledges the technical assistance of Mr. S. T. Spivac and Miss Loh and the financial support from the National Research Council of Canada.

### References

1. I. M. Rozman and K. G. Zimmer, *Int. J. Radiat. Isotopes*, **3**, 36 (1958).
2. I. M. Rozman, *Izv. Akad. Nauk S.S.S.R., Ser. Fiz.*, **22**, 60 (1958).
3. G. Oldham, A. R. Ware, and S. A. Blackwell, *Nucl. Energy*, **20**, 158 (1967).
4. J. Gallocher and N. A. Weir, *Int. J. Radiat. Isotopes*, **23**, 371 (1972).
5. N. Grassie and N. A. Weir, *J. Appl. Polym. Sci.*, **9**, 975 (1965).
6. M. H. Main and N. A. Weir, unpublished data, 1970.
7. G. C. Hatchard and C. A. Parker, *Proc. Roy. Soc.*, **A235**, 518 (1956).
8. S. Stokes and R. B. Fox, *J. Polym. Sci.*, **58**, 507 (1962).
9. W. Burland and J. N. Neeman, *ibid.*, **58**, 491 (1962).
10. A. Charlesby, *Atomic Radiation of Polymers*, Pergamon Press, Oxford, 1960.
11. H. Jacobs and R. Steel, *J. Appl. Polym. Sci.*, **3**, 239 (1960).
12. M. R. Kamal, *Polym. Eng. Sci.*, **10**, 113 (1970).
13. J. B. Lawrence and N. A. Weir, unpublished work, 1969.
14. S. K. Kwei Ping, *J. Appl. Polym. Sci.*, **12**, 1543 (1968).
15. F. Hirayama, *J. Chem. Phys.*, **42**, 3162 (1965).
16. E. A. Chadros and C. J. Dempster, *J. Amer. Chem. Soc.*, **92**, 3568 (1970).
17. M. T. Vala, J. Haebig, and S. A. Rice, *J. Chem. Phys.*, **43**, 886 (1965).
18. R. B. Fox, T. R. Price, J. R. McDonald, and R. F. Cozzens, *Macromolecular Preprints*, **Vol. 1**, 90 (1971).
19. H. L. MacMurray and V. Thornton, *Anal. Chem.*, **24**, 318 (1959).
20. J. Brown, *J. Amer. Chem. Soc.*, **77**, 634, 1955.
21. L. A. Wall and D. W. Brown, *J. Phys. Chem.*, **24**, 318 (1959).
22. S. W. Benson, *Thermochemical Kinetics*, Wiley, New York, 1969.
23. N. Grassie and N. A. Weir, *J. Appl. Polym. Sci.*, **9**, 999 (1965).

Received August 1, 1972